Dispersive force between dissimilar materials: Geometrical effects

Cecilia Noguez* and C. E. Román-Velázquez
Instituto de Física, Universidad Nacional Autónoma de México, Apartado Postal 20-364, D.F. 01000, Mexico
(Received 21 November 2003; revised manuscript received 20 August 2004; published 11 November 2004)

We calculate the Casimir force or dispersive van der Waals force between a spherical nanoparticle and a planar substrate, both with arbitrary dielectric properties. We show that the force between the sphere and half-space can be calculated through the interacting surface plasmons of the bodies. Using a Spectral Representation formalism, we show that the force of a sphere made of a material A and a half-space made of a material B differs from the case when the sphere is made of B, and the half-space is made of A. We find that the difference depends on the plasma frequency of the materials, the geometry, and the distance of separation between the sphere and half-space. The differences show the importance of the geometry, and make evident the necessity of realistic descriptions of the system beyond the Derjaguin Approximation or Proximity Theorem Approximation.

DOI: 10.1103/PhysRevB.70.195412 PACS number(s): 41.20.Cv, 77.55.+f, 02.70.Hm, 12.20.Ds

I. INTRODUCTION

The origin of dispersive forces like Casimir[1] and van der Waals (vW) forces[2,3] between atoms and macroscopic bodies may be attributed to electromagnetic interactions between their charge distributions induced by quantum vacuum fluctuations, even when they are electrically neutral.[1–4] In a first approximation, the charge distribution of neutral particles may be represented by electric dipoles. This dipole approximation was employed by London to calculate the nonretarded van der Waals interaction potential between two identical polarizable molecules by using perturbation theory in quantum mechanics.[5] Later, Casimir studied a simpler problem:[1] the force between two parallel conducting plates separated by a distance z, due to the change of the zero-point energy of the classical electromagnetic modes. He found an interaction energy per unit area, $\mathcal{V}(z)=-(\pi^2\hbar c/720)(1/z^3)$, where c is the speed of light. In 1956, Lifshitz[3] extended the theory of Casimir to dielectric semi-infinite slabs. A decade later, it was shown that the Lifshitz formula could be rederived from the zero-point energy of the surface modes of the slabs.[6–8]

In recent years, accurate experiments[9–13] have been performed to measure the Casimir force, which is one of the macroscopic manifestations of the fluctuations of the quantum vacuum.[1] Most of these experiments[10–13] have been done using a spherical surface and a flat half-space, instead of two parallel plates, as originally proposed Casimir[1] himself. The interpretation of the Casimir force in these experiments is based on the Proximity Theorem which was developed by Derjaguin and collaborators[14] to estimate the force between two curved surfaces of radii R_1 and R_2. The Proximity Theorem or Derjaguin Approximation (DA), which assumes that the force on a small area of one curved surface is due to locally "flat" portions on the other curved surface, gives the force per unit area,

$$\mathcal{F}(z)=2\pi\left(\frac{R_1R_2}{R_1+R_2}\right)\mathcal{V}(z),$$

where $\mathcal{V}(z)$ is the Casimir energy per unit area between parallel plates separated by a distance z. In the limit, when $R_1=R$, and $R_2\to\infty$, the problem reduces to a sphere of radius R and a flat plate, giving $\mathcal{F}(z)=2\pi R\mathcal{V}(z)$. The force obtained using the DA is a power law function of z, and at "large" distances $\mathcal{F}(z)\propto z^{-3}$, while at short distances $\mathcal{F}(z)\propto z^{-2}$. This theorem is supposed to hold when $z\ll R_1,R_2$; however, the validity of the DA has not been proved yet.

Johansonn and Apell[15] studied the vW force between a sphere and a semi-infinite slab. They calculated the electromagnetic stress tensor associated with the electric field correlation of the system from the Green's function of the problem expressed in bispherical coordinates. They concluded that for small separations the behavior of the attractive force is consistent with the DA. However, one drawback of this formalism is that in bispherical coordinates the section surfaces become planar (a point) for small (large) values of z, so it cannot be used to study the system of a sphere and a semi-infinite slab for arbitrary values of z/R.

Casimir showed that the energy $\mathcal{U}(z)$ between two parallel perfect conductor plates can be found from the change of the zero-point energy of the classical electromagnetic field,[1]

$$\mathcal{U}(z)=\frac{\hbar}{2}\sum_i\left[\omega_i(z)-\omega_i(z\to\infty)\right], \tag{1}$$

where $\omega_i(z)$ are the proper modes that satisfy the boundary conditions of the electromagnetic field at the plates which are separated a distance z. For real materials, Lifshitz obtained a formula to calculate the Casimir force between two parallel dielectric half-spaces.[3] The force per unit area, according to the Lifshitz formula, is

$$f(z)=\frac{\hbar c}{2\pi^2}\int_0^\infty dQ\,Q\int_{q\geqslant 0}dk\frac{k^3g}{q}\,\mathrm{Re}\,\frac{1}{\tilde{k}}\left[\frac{1}{\xi^s-1}+\frac{1}{\xi^p-1}\right],$$

with $\xi^\alpha=[r_1^\alpha r_2^\alpha\exp(2i\tilde{k}z)]^{-1}$, where r_j^α is the reflection amplitude coefficient of the half-space j for the electromagnetic field with α-polarization. Here, $\alpha=s$ or p, $q=\omega/c$, ω is the frequency, c is the speed of light, $\vec{q}=(\vec{Q},k)$ is the vacuum wavevector with projections parallel to the surface $\vec{Q}$ and

normal to the surface k, $\tilde{k}=k+i0^+$, and g is the photon occupation number of the state k.

The Lifshitz formula depends only on the reflection coefficients of the plates and the separation between them. These reflection coefficients can be calculated for arbitrary material using the surface impedance formalism for semi-infinite slabs[16–18] and for finite slabs using, for example, the transfer matrix formalism.[19,20] In addition, one observes that the Lifshitz formula is symmetric under the interchange of index $j=1\leftrightarrow 2$; this means that the force is indistinguishable if the half-spaces are exchanged, which is natural given the symmetry of the system.

The force between a sphere and a half-space made of arbitrary dielectric materials is commonly calculated using the DA, where the Casimir energy per unit area $\mathcal{V}(z)$ is found using the Lifshitz formula. As a consequence, the force between a sphere and a half-space is indistinguishable if the sphere is made of a material A and the plate is made of B, or if the sphere is made of B and the plate is made of A. Furthermore, the DA assumes that the interaction of a sphere with a half-space can be calculated as the interaction of a plate with a set of plates, and evaluates the force by adding contributions from various distances, as if the interaction between plates were independent. However, it is well known that the Casimir force is not an additive quantity.[4,21]

In this paper, we show that the geometry of the system is important. We employ a method based on the determination of the proper frequencies of the system based on a spectral representation formalism.[22] By calculating the zero-point energy of all the interacting surface plasmons of a sphere-plate configuration, we find that the force between dissimilar materials differs if the sphere is made of a material A and the plate is made of B, and *vice versa*. This provides an insight into the range of validity of the DA or Proximity Theorem. Also, we find a general formula to calculate the Casimir force differences between arbitrary materials when the bodies are separated by at least one sphere radius. In particular, we study the specific case of aluminum and silver. We restrict ourselves to the nonretarded limit, i.e., to the case of small particles at small distances.

II. ZERO-POINT ENERGY OF INTERACTING SURFACE PLASMONS

A. Parallel plates

In 1968, van Kampen and collaborators[6] showed that the Lifshitz formula in the nonretarded limit is obtained from the zero-point energy of the interacting surface plasmons of the half-spaces. Later, Gerlach[7] did an extension showing that this is also true when retardation is included. A comprehensive derivation of the Lifshitz formula using the surface modes is also found in Ref. 4.

In the case of two parallel plates, in the absence of retardation, the proper electromagnetic modes satisfy the following expression:[6]

$$\left[\frac{\epsilon(\omega)+1}{\epsilon(\omega)-1}\right]^2 \exp[2kz]-1=0, \tag{2}$$

for any value of $0\leqslant k\leqslant\infty$. The roots $\omega_i(k)$ are identified as the oscillation frequencies of the surface plasmons. To find the proper modes, it is necessary to choose a model for the dielectric function of the plates. To illustrate the procedure for metallic plates, let us employ the plasma model for the dielectric function,

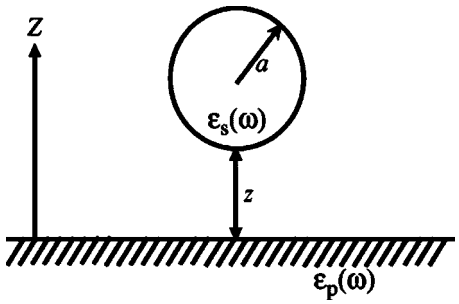

FIG. 1. Schematic model of the sphere-substrate system.

$$\epsilon(\omega)=1-\frac{\omega_p^2}{\omega^2}, \tag{3}$$

with ω_p the plasma frequency. Substituting Eq. (3) in Eq. (2), we find two proper modes that, at large distances ($kd\gg 1$), are given by

$$\omega_\pm \approx \frac{\omega_p}{\sqrt{2}}\left(1\pm\frac{1}{2}\exp[-kd]-\frac{1}{8}\exp[-2kd]\pm\cdots\right). \tag{4}$$

In the limit $kd\to\infty$, we obtain $\omega_\pm=\omega_p/\sqrt{2}$ which are the frequencies of the surface plasmon of each half-space. The zero-point energy per unit area will be given by

$$\mathcal{E}_0(z)=\frac{1}{2}\frac{\hbar\omega_p}{\sqrt{2}}2\pi\int_0^\infty\sum_i\omega_i(k)k\,dk. \tag{5}$$

Now, taking the difference of the zero-point energy when the two half-spaces are at a distance z, and when they are at infinity, we obtain the interaction energy of the system per unit area,

$$\mathcal{V}(z)=-\frac{\hbar\omega_p}{\sqrt{2}}\frac{\pi}{16z^2}, \tag{6}$$

which depends on the energy of the surface plasmons of the half-spaces and the distance between them.

B. Sphere and half-space: Dipolar approximation

Now, let us consider the case of a sphere of radius a and dielectric function $\epsilon_s(\omega)$, such that the sphere is located at a minimum distance z from a half-space with dielectric function $\epsilon_p(\omega)$, as shown in Fig. 1. The quantum vacuum fluctuations will induce a charge distribution on the sphere which also induces a charge distribution in the half-space. Then, the induced lm-th multipolar moment on the sphere is given by[23]

$$Q_{lm}(\omega)=\alpha_{lm}(\omega)[V_{lm}^{\mathrm{vac}}(\omega)+V_{lm}^{\mathrm{sub}}(\omega)], \tag{7}$$

where $V_{lm}^{\mathrm{vac}}(\omega)$ is the field associated with the quantum vacuum fluctuations at the zero-point energy, $V_{lm}^{\mathrm{sub}}(\omega)$ is the induced field due to the presence of the half-space, and

$\alpha_{lm}(\omega)$ is the lm-th polarizability of the sphere.

To illustrate the procedure in detail, first we work in the dipolar approximation, i.e., when $l=1$. In Sec. III, we will calculate the proper modes, taking into account all the high-multipolar charge distributions. Using the method of images, the relation between the dipole moment on the sphere $\vec{p}_s(\omega)$, and the induced dipole moment on the half-space $\vec{p}_p(\omega)$, is

$$\vec{p}_p(\omega) = -\frac{1-\epsilon_p(\omega)}{1+\epsilon_p(\omega)}\mathbb{M}\cdot\vec{p}_s(\omega). \tag{8}$$

Here, $\mathbb{M}=(-1,-1,1)$ is a diagonal matrix whose elements depend on the choice of the coordinate system. From Eq. (7), one finds that the total induced dipole moment on the sphere is

$$\vec{p}_s(\omega) = \alpha(\omega)[\vec{E}^{\text{vac}}(\omega) + \mathbb{T}\cdot\vec{p}_p(\omega)], \tag{9}$$

where the dipoles are coupled by the dipole-dipole interaction tensor,

$$\mathbb{T} = (3\vec{r}\vec{r} - r^2\mathbb{I})/r^5.$$

Here, $\mathbb{I}$ is the identity matrix, and $\vec{r}$ is the vector between the centers of the sphere and the dipole charge distribution on the half-space. From Fig. 1, we find that $\vec{r}=(0,0,2(z+a))$, such that $\mathbb{M}\cdot\mathbb{T}=(-1/r^3,-1/r^3,-2/r^3)$ is a diagonal matrix. Substituting Eq. (8) in Eq. (9), one finds

$$\left[\frac{1}{\alpha(\omega)}\mathbb{I} + f_c(\omega)\mathbb{M}\cdot\mathbb{T}\right]\cdot\vec{p}_s(\omega) = \mathbb{G}(\omega)\cdot\vec{p}_s(\omega) = \vec{E}^{\text{vac}}(\omega), \tag{10}$$

where

$$f_c(\omega) = [1-\epsilon_p(\omega)]/[1+\epsilon_p(\omega)].$$

Multiplying Eq. (10) by a^3, one finds that each term of $a^3\mathbb{G}(\omega)$ is dimensionless and has two parts: the first part is only associated with the material properties of the sphere through its polarizability $1/\tilde{\alpha}(\omega)=a^3/\alpha(\omega)$. The second part is related to the geometrical properties of the system a, and z, and also depends on the dielectric properties of the half-space.

The eigenfrequencies of the sphere-substrate system must satisfy Eq. (10), and are independent of the exciting field, $\vec{E}^{\text{vac}}(\omega)$. These frequencies can be obtained from the condition $\det\mathbb{G}(\omega)=0$, or

$$\left[\frac{1}{\tilde{\alpha}(\omega)} + \frac{f_c(\omega)a^3}{[2(z+a)]^3}\right]^2\left[\frac{1}{\tilde{\alpha}(\omega)} + \frac{2f_c(\omega)a^3}{[2(z+a)]^3}\right] = 0. \tag{11}$$

In the dipolar approximation, we find three terms, one for each independent coordinate of the system. Given the symmetry of the system, the factors belong to the x and y directions (parallel to the surface) are doubly degenerated. The second factor belongs to the z direction (normal to the surface).[22] At this point, it is necessary to consider a model for the dielectric function of the sphere to find the proper modes. Again, we illustrate the procedure for a metallic sphere and a half-space of the same material, with $\epsilon_p(\omega)=\epsilon_s(\omega)=\epsilon(\omega)$ from Eq. (3). Moreover, we use the fact that

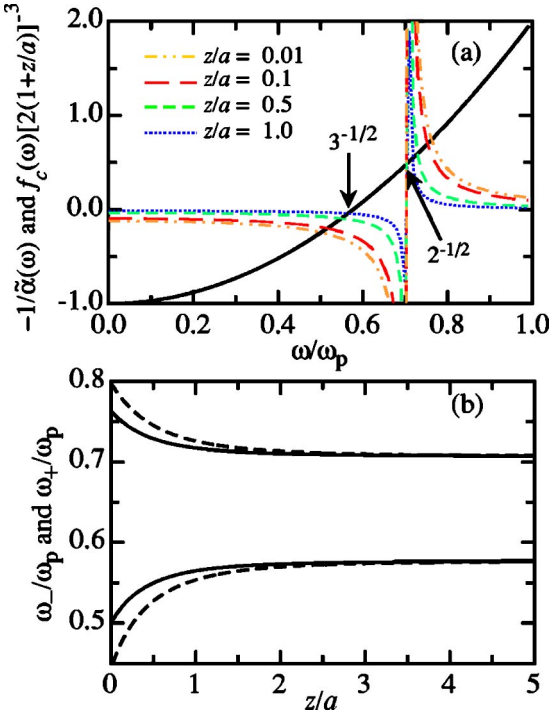

FIG. 2. (Color online) (a) Plot of $-1/\tilde{\alpha}(\omega)$ in solid line and $f_c(\omega)[2(1+z/a)]^{-3}$ as a function of ω/ω_p for different values of z/a. (b) Proper modes ω_+ and ω_- as a function of z/a.

the polarizability of the sphere, within the dipolar approximation and in the quasi-static limit, is given by

$$\alpha(\omega) = a^3\frac{\epsilon_s(\omega)-1}{\epsilon_s(\omega)+2}.$$

Then, we find that there are two different proper modes for each factor in Eq. (11), giving a total of six modes for each z/a. The modes associated with the directions on the surface plane of the half-space are degenerated.

In Fig. 2(a), we plot, $-1/\tilde{\alpha}(\omega)$ and $f_c(\omega)[2(1+z/a)]^{-3}$ as a function of ω/ω_p for different values of z/a. The proper frequencies of the system are given when the black-solid line and the color-dashed lines intersect each other. The proper modes at the left-hand side in Fig. 2(a) correspond to the surface plasmons of the sphere that we denote with ω_+. These modes are red-shifted as the sphere approaches the half-space because of the interaction between bodies. When the separation z/a increases, the modes ω_+ go to $\omega_p/\sqrt{3}$, which is the surface plasmon frequency of an isolated sphere. On the other hand, the proper modes at the right-hand side correspond to the surface plasmons of the half-space and we denote them with ω_-. These modes are blue-shifted as the sphere approaches the half-space, also because of the interaction between the sphere and the half-space. In this case, when the separation z/a increases, the mode ω_- goes to $\omega_p/\sqrt{2}$, which corresponds to the frequency of the surface plasmon of the isolated half-space. This behavior of the modes is clearly observed in Fig. 2(b), where ω_+/ω_p and ω_-/ω_p are plotted as a function of z/a for both factors in Eq. (11). The modes associate to the left-hand side factor are

plotted in a solid line, while the modes associate to the right-hand factor are plotted in a dashed line. This shows that the zero-point energy of the system is directly associated with the interacting surface plasmons of the sphere and the half-space.

III. EXACT CALCULATION OF THE ZERO-POINT ENERGY OF A SPHERE ABOVE A HALF-SPACE

In this section we calculate the proper electromagnetic modes of the sphere-substrate system, within the nonretarded limit, including all the high-multipolar interactions. We find these proper modes using a Spectral Representation formalism,[24–26] and then, we calculate the zero-point energy using Eq. (1). The Spectral Representation (SR) formalism separates the contributions of the dielectric properties of the sphere from the contributions of its geometrical properties. This separation has advantages over other formalisms and allows us to perform a systematic study of the sphere-substrate system that may be very helpful. The details of the SR formalism can be found in Refs. 22 and 27; here we only explain it briefly.

We now calculate the proper modes of the system including all the high-multipolar charge distributions. Using the method of images, we find that Eq. (7) becomes

$$-\sum_{l'm'}\left[\frac{4\pi\delta_{ll'}\delta_{mm'}}{(2l+1)\alpha_{l'm'}(\omega)}+f_c(\omega)A_{lm}^{l'm'}(z)\right]Q_{l'm'}(\omega)=V_{lm}^{\mathrm{vac}}(\omega), \tag{12}$$

where $A_{lm}^{l'm'}(z)$ is the matrix that describes the interaction between sphere and its image.[23] The expression for the interaction matrix $A_{lm}^{l'm'}(z)$ is given in the Appendix, and it shows that $A_{lm}^{l'm'}(z)$ depends only on the geometrical properties of the system. If we have a homogeneous sphere, its polarizabilities are independent of the index m, and are given by[23]

$$\alpha_l(\omega)=\frac{l[\epsilon_s(\omega)-1]}{l[\epsilon_s(\omega)+1]+1}a^{2l+1}=\frac{n_{l0}}{n_{l0}-u(\omega)}a^{2l+1}, \tag{13}$$

where $n_{l0}=l/(2l+1)$, and $u(\omega)=[1-\epsilon_s(\omega)]^{-1}$. Notice that in the above equation for the polarizability, the dielectric properties of the sphere are separated from its geometrical properties. By substituting the right-hand side of the above equation, we rewrite Eq. (12) as

$$\sum_{l'm'}\{-u(\omega)\delta_{ll'}\delta_{mm'}+H_{lm}^{l'm'}(\omega,z)\}\frac{Q_{l'm'}(\omega)}{(l'a^{2l'+1})^{1/2}}=-\frac{(la^{2l+1})^{1/2}}{4\pi}V_{lm}^{\mathrm{vac}}(\omega), \tag{14}$$

where the $lm,l'm'$-th element of the matrix $\mathbb{H}(\omega,z)$ is

$$H_{lm}^{l'm'}(\omega,z)=n_{l'0}\delta_{ll'}\delta_{mm'}+f_c(\omega)\frac{(a^{l+l'+1})}{4\pi}(ll')^{1/2}A_{lm}^{l'm'}(z). \tag{15}$$

The proper modes are given when the determinant of the quantity between parentheses in Eq. (14) is equal to zero, $\det[-u(\omega)\mathbb{I}+\mathbb{H}(\omega,z)]=0$, that is

$$G(\omega,z)\equiv\prod_s[-u(\omega)+n_s(\omega,z)]=0, \tag{16}$$

where $n_s(\omega,z)$ are the eigenvalues of $\mathbb{H}(\omega,z)$. The frequencies of the proper modes at z are found from the last equation.

The Spectral Representation formalism can be applied in a very simple way. First, we have to choose a substrate to calculate the factor $f_c(\omega)$, we then construct the matrix $\mathbb{H}(\omega,z)$, and diagonalize it to find its eigenvalues $n_s(\omega,z)$. We can repeat these steps for a set of different values of z and ω. Notice that the eigenvalues of $\mathbb{H}(\omega,z)$ can be found without making any assumption about the dielectric function of the sphere. Once we have the eigenvalues as a function of z and ω, we have to consider an explicit form of the dielectric function of the sphere, and calculate the proper mode frequencies $\omega_s(z)$ from Eq. (16) through the relation $u(\omega_s)=n(\omega_s,z)$.

To illustrate the procedure, we consider the case where the sphere and the half-space are both described by the plasma model of the same plasma frequency. The frequencies of the proper modes are given by

$$\omega_s(z)=\omega_p\sqrt{n_s(\omega_s(z),z)}, \tag{17}$$

with $s=(l,m)$, and $n_s(\omega_s(z),z)$ the eigenvalues of $\mathbb{H}(\omega,z)$. Then, the zero-point energy, in accordance with Eq. (1), is given by

$$\mathcal{U}(z)=\frac{\hbar\omega_p}{2}\sum_{l,m}[\sqrt{n_{lm}(\omega_s(z),z)}-\sqrt{n_{l0}}], \tag{18}$$

where $\hbar\omega_p\sqrt{n_{l0}}=\hbar\omega_p\sqrt{l/(2l+1)}$ are the energies associated with the multipolar surface plasmon resonances of the isolated sphere. These modes are found when $z\to\infty$, such that the second term of Eq. (15) is zero. Here, $l=1,2,\ldots,L$, where L is the largest order in the multipolar expansion. For $l=1$ we have that $\hbar\omega_p\sqrt{n_{10}}=\hbar\omega_p/\sqrt{3}$ is the surface plasmon of the sphere in the dipolar approximation. When $l\to\infty$, we have $\hbar\omega_p\sqrt{n_{l0}}\to\hbar\omega_p/\sqrt{2}$, the surface plasmon of a half-space.

Now, in the presence of a dielectric half-space, the proper modes of the sphere are given diagonalizing Eq. (15). These proper modes are red-shifted always as the sphere approaches the half-space, and this shift depends on the separation z/a. We find that the interaction energy is proportional to $[1/2(1+z/a)]^{\beta}$, where $\beta=l+l'+1$ is an integer between 3 and $2L+1$. As $z/a\to0$, more and more multipolar interactions must be taken into account and $\beta\to2L+1$. Finally, when the sphere is touching the substrate, one would expect that $L\to\infty$, so that also $\beta\to\infty$, and the energy at $z=0$ is proportional to $(1/2)^{\gamma}$, with $\gamma\to\infty$.

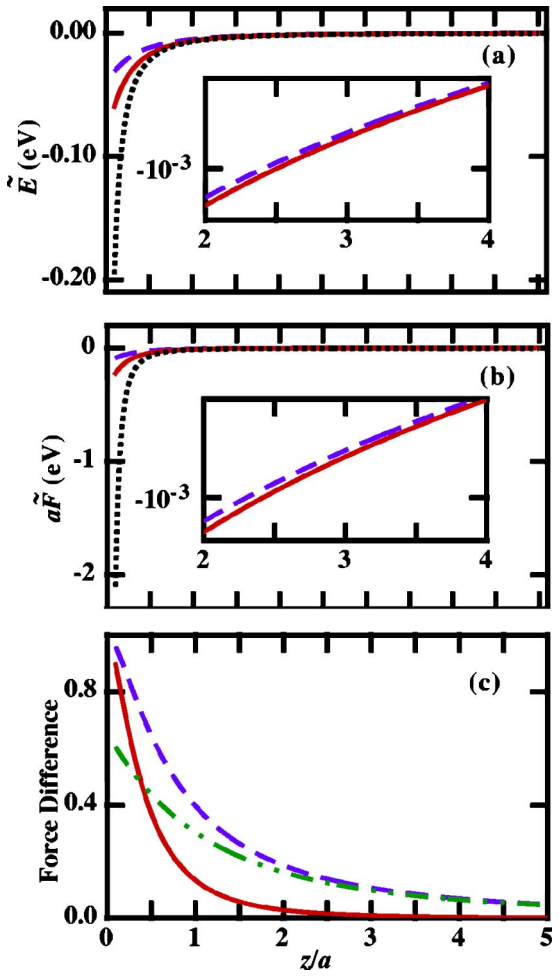

FIG. 3. (Color online) (a) Energy $\tilde{\mathcal{E}}$ and (b) force $a\tilde{F}$ as a function of z/a, with $L=80$ (dotted line), $L=2$ (solid line), and $L=1$ (dashed line). (c) Force difference, $|(\tilde{F}^{LH}-\tilde{F}^{LW})/\tilde{F}^{LH}|$, using multipolar moments $LH=80$ and $LW=2$ (solid line), $LH=80$ and $LW=1$ (dashed line), finally $LH=2$ and $LW=1$ (dot-dot-dashed line).

From Eq. (18), we find that the behavior of the energy as a function of z/a is proportional to the plasma frequency of the sphere. Then, we can define a dimensionless quantity $\tilde{\mathcal{E}} \equiv \mathcal{U}/\hbar\omega_p$. The force along the z axis is

$$F = -\frac{\partial \mathcal{U}(z/a)}{\partial z} = -\frac{\partial \mathcal{U}(z/a)}{\partial (z/a)}\frac{\partial (z/a)}{\partial z}. \tag{19}$$

Therefore, the behavior of the force can also be studied using a quantity independent of the radius of the sphere, and of its plasma frequency. We define a dimensionless force as $\tilde{F} \equiv aF/\hbar\omega_p$. In summary, we find a general behavior of the energy and force between a half-space and a sphere, showing the potentiality of the Spectral Representation formalism.[22]

In the same way, we find the dimensionless energy and force for a system composed of a sphere and a half-space of similar materials, whose dielectric function is described by the plasma model of Eq. (3). In Figs. 3(a) and 3(b), we show $\tilde{\mathcal{E}}$, and $\tilde{F}$, respectively, as a function of z/a. In each figure we show three curves that correspond to three different situations: (i) when all multipolar interactions are taken into account, (ii) when only dipolar $(L=1)$, and (iii) when up to quadrupolar $(L=2)$ interactions are considered. The largest multipolar moment to achieve convergence of the energy at a minimum separation of $z/a=0.1$ is $L=80$. We observe that $\tilde{\mathcal{E}}$ and $a\tilde{F}$ are power law functions of $(z/a)^{-\beta}$, where β depends on the order of the multipolar interaction considered. Within the dipolar approximation $\tilde{\mathcal{E}}$ and $\tilde{F}a$ are proportional to $(z/a)^{-3}$, and $(z/a)^{-4}$, respectively. Let us first analyze the system when up to quadrupolar interactions are taken into account. In that case, the energy as well as the force show three different regions: (i) at large distances, $z>5a$, only dipolar interactions are important; (ii) when $5a>z>2a$, we found that dipolar-quadrupolar interactions become important and $\tilde{\mathcal{E}}$ and $\tilde{F}a$ are proportional to $(z/a)^{-4}$, and $(z/a)^{-5}$ respectively; while (iii) at small distances $z<2a$ the quadrupolar-quadrupolar interaction dominates, and $\tilde{\mathcal{E}}$ and $\tilde{F}a$ like $(z/a)^{-5}$, and $(z/a)^{-6}$, respectively.

When the sphere approaches the substrate the interaction between high-multipolar moments becomes more and more important. The attractive force increases more than four orders of magnitude, as compared with the dipolar and quadrupolar approximations. In Fig. 3(c) we show the difference of the dimensionless force, $|(\tilde{F}^{LH}-\tilde{F}^{LW})/\tilde{F}^{LH}|$, as a function of the separation, with LH and LW the highest and lowest-multipolar moments taken into account. Here, we show three curves corresponding to $LH=80$ and $LW=2$ (solid line), $LH=80$ and $LW=1$ (dashed line) and, $LH=2$ and $LW=1$ (dot-dot-dashed line). We observe that at distances $z>2a$ the force can be obtained if up to quadrupolar interactions are considered. We also find that for $z>7a$ the interaction between the sphere and the substrate can be modeled using the dipolar approximation only, like in the Casimir and Polder model.[28] However, at separations smaller than $z<2a$, the quadrupolar approximation also fails, and it is necessary to include high-multipolar contributions. For example, at $z=a$ the quadrupolar approximation gives an error of about 10%, while the dipolar approximation gives an error of about 40%. At smaller distances like $z=a/2$, the quadrupolar approximation gives an error of about 40%, while in the dipolar approximation the error is 70%. At $z=0.1a$ both approximations give an error larger than 90%. To directly compare the dipolar and quadrupolar approximations, we also plot in Fig. 3(c) the force difference when $LH=2$ and $LW=1$. In this curve, we clearly observe that even at $z=5a$ there are differences between the dipolar and quadrupolar approximations of about 5%.

The large increment of the force at small separations due to high-multipolar effects could explain the physical origin of, for example, the large deviations observed in the deflection of atomic beams by metallic surfaces,[29] as well as some instabilities detected in micro and nano devices. Furthermore, to compare experimental data of some experiments[12,30] with the DA, it is necessary to make a significant modification to the theory of the Casimir force. In Ref. 12 the authors found a larger force than the one calculated using DA, while in Ref. 30 the authors measured a smaller one. Both groups argue that the discrepancies between theory and experiment

are due to the same effect: the roughness of the surface. Indeed, this ambiguity on the interpretation of the measurements indicates that the force between a spherical particle and a planar substrate involves more complicated interactions than the simple dipole model[28] or the DA.[14] For example, such deviations might be attributed also to high-multipolar effects.

In this paper, we propose a way to elucidate experimentally two important issues related to the Casimir force: (i) the relevance of the geometry via the surface plasmon interactions between bodies, and (ii) the relevance of the high-multipolar interactions in the sphere-substrate model. In the next section, we study the case of the Casimir force between a sphere and a half-space of dissimilar materials that can help us to clarify these important issues.

IV. CASIMIR FORCE BETWEEN DISSIMILAR MATERIALS

Using the formalism presented in the previous section, we calculate the Casimir force for a sphere and a half-space made of dissimilar materials. To illustrate our results, we choose silver (Ag) and aluminum (Al) whose dielectric functions are described by the Drude model,

$$\epsilon(\omega) = 1 - \frac{\omega_p^2}{\omega(\omega + i/\tau)}, \tag{20}$$

with plasma frequencies $\hbar\omega_p = 9.6$ eV, and 15.8 eV, and $(\tau\omega_p)^{-1} = 0.0019$, and 0.04, respectively.[32] If the materials have dielectric functions with nonzero imaginary parts, the mode frequencies are complex and the direct sum of $\omega_s(z)$, to calculate the energy on Eq. (1), is not valid. However, we can employ the Argument Principle (AP) to calculate the energy as follows. The AP was first used by van Kampen[6] and Gerlach[7] to calculate the force between plates. The reader can consult Ref. 4 for a comprehensive explanation of the use of the AP within the context of Casimir forces.

According to the Argument Principle method, the sum over proper modes is given as

$$\mathcal{E}(z) = \sum_s \frac{\hbar\omega_s(z)}{2} = \frac{\hbar}{4\pi i}\oint_C \omega \frac{\partial G(\omega,z)}{\partial\omega}\frac{1}{G(\omega,z)}d\omega, \tag{21}$$

using the expression for $G(\omega,z)$ in Eq. (16), we find that

$$\mathcal{E}(z) = \frac{\hbar}{4\pi i}\sum_s \oint_C \omega \frac{\partial}{\partial\omega}\log[-u(\omega) + n_s(\omega,z)]d\omega. \tag{22}$$

The closed contour C is defined as the part along the imaginary axis plus the part along the semicircle on the positive real axis. In the limit of an infinite semicircle radius, the integral along the semicircle does not depend on the separation z; therefore, it does not contribute to the force. The integral in Eq. (21) is along the imaginary ω axis, so the dielectric functions are real, the matrix $\mathbb{H}$ defined by Eq. (15) is Hermitian and has real eigenvalues, giving a real energy. By performing a partial integration, it follows that the interaction energy of Eq. (1) is given by

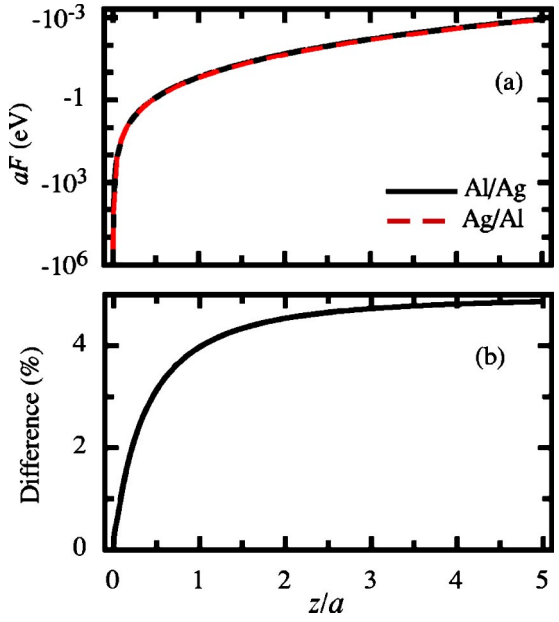

FIG. 4. (Color online) (a) Force as a function of z/a, for a sphere made of Al over an Ag plane (solid line), and for a sphere made of Ag over an Al substrate (dashed line). (b) Difference of the force between a sphere made of Al over an Ag substrate, and the force for a sphere made of Ag over an Al substrate.

$$\begin{aligned}\mathcal{U}(z) &= \frac{\hbar}{2}\sum_i [\omega_i(z) - \omega_i(z\to\infty)] \\ &= \frac{\hbar}{4\pi i}\sum_s \int_{-i\infty}^{i\infty} d\omega \log[-u(\omega) + n_s(\omega,z)] \\ &\quad - \frac{\hbar}{4\pi i}\sum_l \int_{-i\infty}^{i\infty} d\omega \log[-u(\omega) + n_{l0}].\end{aligned} \tag{23}$$

The force is found as in Eq. (19), where we first find the derivative of Eq. (23) with respect to z and then the integral with respect to ω. Notice that the last term of Eq. (23) does not contribute to the force because it does not depend on the separation z.

In Fig. 4(a), we show the calculated force for an aluminum sphere of arbitrary radius above a silver half-space, $aF_{\mathrm{Al/Ag}}$, as a solid line, and the same for a silver sphere above an aluminum half-space, $aF_{\mathrm{Ag/Al}}$, as a dashed line. We find that the difference is too small to be observed directly from the figure. Then, in Fig. 4(b) we show the difference of the force normalized with the average as a function of z/a, given by

$$\Delta\mathcal{F} = 2\left|\frac{F_{\mathrm{A/B}} - F_{\mathrm{B/A}}}{F_{\mathrm{A/B}} + F_{\mathrm{B/A}}}\right|, \tag{24}$$

with A = Al, and B = Ag. Here, we observe that the difference of force varies as a function of z/a, such that at small distances ($z < 0.5a$), the difference under the interchange of materials between the sphere and the plane, is less than 3%. Then, the difference increases as the separation is increased, and at $z > a$, it has almost reached its maximum. For these

particular materials, the maximum is about 5%, independent of the radius of the sphere. We find that this value of $\Delta\mathcal{F}$ is a consequence of the geometry of the system, as we explain below.

In the previous section, we show that for a minimum separation larger than $2a$, the force can be described with quadrupolar interactions between the sphere and the substrate. This means that for $z>2a$ the force varies with the same power-law function. This conclusion can be easily found from Fig. 3(c). We also show in Sec. II that the Casimir force is given by the interaction of the surface plasmons of the sphere and plane. In Fig. 2(b), we observe that the proper modes of the system for $z>a$ are approximately given by $\hbar\omega_p/\sqrt{2}$ and $\hbar\omega_p/\sqrt{3}$, when $L=1$. It follows that for $z>a$, the force difference is independent of z, and has the value

$$\Delta\mathcal{F}\simeq 2\left|\frac{\left(\frac{\hbar\omega_p^{\mathrm{A}}}{\sqrt{3}}+\frac{\hbar\omega_p^{\mathrm{B}}}{\sqrt{2}}\right)-\left(\frac{\hbar\omega_p^{\mathrm{B}}}{\sqrt{3}}+\frac{\hbar\omega_p^{\mathrm{A}}}{\sqrt{2}}\right)}{\left(\frac{\hbar\omega_p^{\mathrm{A}}}{\sqrt{3}}+\frac{\hbar\omega_p^{\mathrm{B}}}{\sqrt{2}}\right)+\left(\frac{\hbar\omega_p^{\mathrm{B}}}{\sqrt{3}}+\frac{\hbar\omega_p^{\mathrm{A}}}{\sqrt{2}}\right)}\right|,$$

$$=0.202\left|\frac{\hbar\omega_p^{\mathrm{A}}-\hbar\omega_p^{\mathrm{B}}}{\hbar\omega_p^{\mathrm{A}}+\hbar\omega_p^{\mathrm{B}}}\right|. \tag{25}$$

For the case of A=Al, and B=Ag, we find from Eq. (25) that $\Delta\mathcal{F}\simeq 5\%$, which is the calculated value shown in Fig. 4(b) when $z>2a$. When $z<a$ the difference decreases as z/a also does, because more and more multipolar interactions become important as the sphere approaches the plane. In the case of Al and Ag, the force difference at $z/a=0.001$ is less than 0.01%, while at $z/a=0.1$ the difference is about 1.2%. At $z/a=0.001$ we take $L=1300$ to achieve convergency on the values of the force. In Eq. (25) we observe that as the plasma frequency of the materials becomes more dissimilar the difference of the force becomes larger. For example, for potassium ($\hbar\omega_p=3.8$ eV) and aluminum we would find that $\Delta\mathcal{F}\simeq 12.4\%$ when $z>2a$, while for gold ($\hbar\omega_p=8.55$ eV) and copper ($\hbar\omega_p=10.8$ eV), $\Delta\mathcal{F}\simeq 2.4\%$ when $z>2a$. On the other hand, the differences become very small when $z<0.1a$ independently of the materials because of the dominant terms on the force are due to interactions between high-multipolar surface plasmon which eigenvalues are very similar for large values of L, so the force is almost unchangedif the materials of the bodies are changed.

V. SUMMARY

In this work, we show that the Casimir force between a sphere and a plane can be calculated through the energy obtained from their interacting surface plasmons. Our result is in agreement with the work of van Kampen and collaborators,[6] and Gerlach,[7] which showed that the Casimir force between parallel planes can be obtained from the zero-point energy of the interacting surface plasmons of the planes. We show that the Casimir force of a sphere made of a given material A and a plane made of a given material B, is different from the case when the sphere is made of B, and the plane is made of A. We obtain a formula to estimate the force difference for Drude-like materials, when they are separated by at least two sphere radii. We find that the difference depends on (i) the plasma frequencies of the materials, and (ii) the distance of separation between the sphere and the plane. We also find that as the sphere approaches the plane, the force difference becomes smaller. We conclude that the geometry of the system is important at distances larger than the radius of the sphere, where the force is dominated by the surface plasmons of the bodies. The energy of these surface plasmons is equal to the plasma frequencies of the materials times a factor given by the geometry.

ACKNOWLEDGMENTS

We would like to thank Raúl Esquivel-Sirvent and Rubén G. Barrera for helpful discussions. This work has been partly financed by CONACyT Grant No. 36651-E and by DGAPA-UNAM Grant No. IN104201.

APPENDIX: MULTIPOLAR INTERACTION MATRIX

The tensor that couples the sphere and its image is[23]

$$A_{lm}^{l'm'}=\frac{Y_{l+l'}^{m-m'}(\theta,\varphi)}{r^{l+l'+1}}\left[\frac{(4\pi)^3(l+l'+m-m')!\,(l+l'-m+m')!}{(2l+1)(2l'+1)(2l+2l'+1)(l+m)!\,(l-m)!\,(l'+m')!\,(l'-m')!}\right]^{1/2} \tag{A1}$$

where $Y_{lm}(\theta,\varphi)$ are the spherical harmonics. In spherical coordinates $\vec{r}=(2(z+a),0,0)$, so the spherical harmonics reduce to[31]

$$Y_{l+l'}^{m-m'}(0,\varphi)=\left[\frac{2(l+l')+1}{4\pi}\right]^{1/2}\delta_{m-m',0}. \tag{A2}$$

This means that $m=m'$ and multipolar moments with different azimuthal charge distribution are not able to interact. Therefore,

$$A_{lm}^{l'm'}=\frac{4\pi}{[2(z+a)]^{l+l'+1}}\left[\frac{((l+l')!)^2}{(2l+1)(2l'+1)(l+m)!\,(l-m)!\,(l'+m)!\,(l'-m)!}\right]^{1/2}\delta_{mm'}, \tag{A3}$$

which is a symmetric matrix.

*Corresponding author. Electronic address: cecilia@fisica.unam.mx

[1] H. B. G. Casimir, Proc. K. Ned. Akad. Wet. **51**, 793 (1948).
[2] I. E. Dzyaloshinskii, E. M. Lifshitz, and L. P. Pitaevskii, Sov. Phys. Usp. **73**, 153 (1961).
[3] E. M. Lifshitz, Sov. Phys. JETP **2**, 73 (1956).
[4] P. W. Milonni, *The Quantum Vacuum, An Introduction to Quantum Electrodynamics* (Academic Press, San Diego, 1994).
[5] F. London, Trans. Faraday Soc. **32**, 10 (1937).
[6] N. G. van Kampen, B. R. A. Nijboer, and K. Schram, Phys. Lett. A **26**, 307 (1968).
[7] E. Gerlach, Phys. Rev. B **4**, 393 (1971).
[8] Y. S. Barash and V. L. Ginzburg, Sov. Phys. Usp. **18**, 305 (1975).
[9] G. Bressi, G. Carugno, R. Onofrio, and G. Ruoso, Phys. Rev. Lett. **88**, 041804 (2002).
[10] S. K. Lamoreaux, Phys. Rev. Lett. **78**, 5 (1997).
[11] U. Mohideen and A. Roy, Phys. Rev. Lett. **81**, 4549 (1998).
[12] H. B. Chan, V. A. Aksyuk, R. N. Kliman, D. J. Bishop, and F. Capasso, Science **291**, 1942 (2001).
[13] R. Decca, D. López, E. Fischbach, and D. Krause, Phys. Rev. Lett. **91**, 050402 (2003).
[14] B. Derjaguin and I. Abrikosova, Sov. Phys. JETP **3**, 819 (1957).
[15] P. Johansson and P. Apell, Phys. Rev. B **56**, 4159 (1997).
[16] R. Esquivel-Sirvent, C. Villarreal, W. L. Mochán, and G. H. Cocoletzi, Phys. Status Solidi B **230**, 409 (2002).
[17] W. L. Mochán, C. Villarreal, and R. Esquivel-Sirvent, Rev. Mex. Fis. **48**, 339 (2002).
[18] R. Esquivel-Sirvent, C. Villarreal, and W. L. Mochán, Phys. Rev. A **68**, 052103 (2003).
[19] R. Esquivel-Sirvent, C. Villarreal, and G. H. Cocoletzi, Phys. Rev. A **64**, 052108 (2001).
[20] R. Esquivel-Sirvent, C. Villarreal, and G. H. Cocoletzi, Int. J. Mod. Phys. A **17**, 798 (2002).
[21] A. Lambrecht and S. Reynaud, Eur. Phys. J. D **8**, 309 (2000).
[22] C. E. Román-Velázquez, C. Noguez, C. Villarreal, and R. Esquivel-Sirvent, Phys. Rev. A **69**, 042109 (2004).
[23] F. Claro, Phys. Rev. B **30**, 4989 (1984).
[24] R. Fuchs, Phys. Rev. B **11**, 1732 (1975).
[25] D. J. Bergman, Phys. Rev. B **19**, 2359 (1979).
[26] G. W. Milton, Appl. Phys. Lett. **37**, 300 (1980).
[27] C. Noguez, C. E. Román-Velázquez, R. Esquivel-Sirvent, and C. Villarreal, Europhys. Lett. **67**, 191 (2004).
[28] H. B. G. Casimir and D. Polder, Phys. Rev. **73**, 360 (1948).
[29] A. Shih and V. A. Parsegian, Phys. Rev. A **12**, 835 (1975).
[30] R. Decca, E. Fischbach, G. L. Klimchitskaya, D. E. Krause, D. López, and V. M. Mostepanenko, Phys. Rev. D **68**, 116003 (2003).
[31] G. Arfken, *Mathematical Methods for Physicists* (Academic Press, San Diego, 1985), 3rd ed.
[32] We employ the Drude parameters that were found for small silver particles by U. Kreibig, [J. Phys. F: Met. Phys. **4**, 499 (1974)]. However, there is no consensus on the values of the plasma frequency and relaxation time for silver. The value of these parameters depend on temperature and other experimental conditions. Therefore, to compare the calculated force with experimental results it would be necessary to measured also the optical response of the sphere and the half-space. However, we hope that the work presented here will stimulate future measurements.